Letter

Experimental investigation of conditional majorization uncertainty relations in the presence of quantum memory

Gaoyan Zhu,[1] Aoxiang Liu,[2] Lei Xiao,[3,1] Kunkun Wang,[4] Dengke Qu,[1] Junli Li,[2,*] Congfeng Qiao,[2,†] and Peng Xue[3,1,‡]

[1]*Beijing Computational Science Research Center, Beijing 100084, China*

[2]*School of Physical Sciences, University of Chinese Academy of Sciences, Beijing 100049, China*

[3]*School of Physics, Southeast University, Nanjing 211189, China*

[4]*School of Physics and Optoelectronics Engineering, Anhui University, Hefei 230601, China*

(Received 14 February 2022; revised 11 May 2023; accepted 19 October 2023; published 7 November 2023)

We report an experimental investigation of conditional majorization uncertainty relations (CMURs) in the presence of quantum memory. We find that the CMUR bounds are always physically nontrivial even if the particle of interest is strongly entangled with a quantum memory, whereas the previous conditional entropic uncertainty relation bounds may be trivial and physically unreachable. We deploy vectorized measures of uncertainty relations and quantum correlations, and the result reveals the sophisticated structures of them. In addition, we demonstrate an application of the CMURs, to witness steerability of bipartite states. Such a method applies to an arbitrary number of measurement settings and can be efficiently implemented. Aside from the CMURs' fundamental significance, our result also shows its impact on the development of future quantum technologies.

DOI: 10.1103/PhysRevA.108.L050202

Introduction. The uncertainty relation, which restricts the uncertainties of the outcomes of two incompatible measurements, is one of the basic principles of quantum mechanics. The uncertainty relation clearly illustrates the fundamental difference between classical and quantum physics. The best-known one is the variance uncertainty relation (Heisenberg-Robertson uncertainty relation) [1–7], which is expressed in terms of the commutator,

$$\triangle X^2 \triangle Y^2 \geqslant \tfrac{1}{4}|\langle [X,Y]\rangle|^2, \tag{1}$$

where $\triangle X^2 (\triangle Y^2)$ represents the variance of the observable $X(Y)$.

The lower bound on the right-hand side (rhs) of (1) is state dependent and can be 0 even for noncommuting observables, which makes the relation trivial. An entropic uncertainty relation [8–10] overcomes this defect, which is expressed as

$$H(X) + H(Y) \geqslant \log_2 \frac{1}{c}, \tag{2}$$

where $H(X)$ denotes the Shannon entropy of measurement probability distribution of observable X; $c \equiv \max_{ij} |\langle x_i|y_j\rangle|^2$ quantifies the complementarity of the two observables, with $|x_i\rangle$ ($|y_j\rangle$) being the eigenvectors of X (Y).

By introducing quantum entanglement, the uncertainty relation in the presence of quantum memory has been proposed [11,12] and experimentally demonstrated that the previous bounds of the uncertainties about the outcomes of two incompatible measurements on a particle can be violated [13–16]. With the particle of interest (A) initially entangled with another particle (B) which acts as a quantum memory, this stronger, conditional entropic uncertainty relation (CEUR) [12] reads as

$$S(X|B) + S(Y|B) \geqslant \log_2 \frac{1}{c} + S(A|B), \tag{3}$$

where $S(X|B)$ [$S(Y|B)$] is the conditional von Neumann entropy representing the uncertainty of the measurement of $X(Y)$ with access to the quantum memory B; $S(A|B)$ is a *negative* conditional entropy which quantifies the effect of the entanglement [17]. Therefore, the CEUR bound depends on the amount of the entanglement between the particle A and the quantum memory B [12].

If A and B are strongly entangled, the CEUR bound may be negative. [Consider a concrete case, where A and B share a maximally entangled state. We then have $S(A|B) = -\log_2 d$ with d representing the dimension of A. The term $\log_2 \frac{1}{c}$ cannot exceed $\log_2 d$, leading to a negative rhs of (3).] Then relation (3) reduces to $S(X|B) + S(Y|B) \geqslant 0$ which is trivial, because the left-hand side (lhs) (that represents the conditional entropy of a system after measurement in the presence of quantum memory) cannot be negative.

In addition, the idea that majorization techniques can be used to quantify uncertainties has been proposed [18], giving the so-called universal uncertainty relations [19–22]. Majorization is a mathematical concept for determining whether a probability distribution is more disordered or spread than another. Majorization $\vec{a} \prec \vec{b}$ is defined as $\sum_{i=1}^{k} a_i^{\downarrow} \leqslant \sum_{j=1}^{k} b_j^{\downarrow}$, $k \in \{1, 2, \ldots, N\}$ for two vectors with elements in descending order and the equality holds for $k = N$. In Ref. [22], Li *et al.*

*Deceased.

†qiaocf@ucas.ac.cn

‡gnep.eux@gmail.com

proposed the optimal universal uncertainty relation in the form of direct-sum majorization,

$$\vec{p}(x) \oplus \vec{p}(y) \prec \vec{s}, \tag{4}$$

where vector $\vec{p}(x)$ [$\vec{p}(y)$] represents the measurement probability distribution of X (Y). Unlike variance- and entropy-based uncertainty relations, an optimal upper bound $\vec{s}$ of (4) can be easily determined with a majorization technique [22,23].

More recently, by virtue of the majorization lattice theory [23], a practical method to reduce the measurement uncertainty of A by determining the measurement on B of an entangled bipartite system is proposed [24]. In light of this method, a family of conditional majorization uncertainty relations (CMURs) in the presence of quantum memory has been constructed [22].

In this Letter, we report an experimental investigation of CMURs with quantum memory in a photonic system. Compared to the previous works that studied uncertainty relations with scalar measures (i.e., variance and entropy), we provide a vectorized measure of quantum uncertainty and quantum correlations in a lattice-structured fashion. Most importantly, we experimentally show that the CMUR bound is nontrivial and physically reachable even if the particle is strongly entangled with another which acts as a quantum memory, while in the same situation, the bound of the conditional entropic uncertainty relation (3) is mostly trivial and physically unreachable. Furthermore, we demonstrate the CMUR's advantages in exploiting the experimentally feasible steering criterion. With a straightforward optimal strategy based on the majorization technique, the criterion can be efficiently implemented with an arbitrary number of measurement settings.

Conditional majorization uncertainty relations. Now we study the uncertainty relations in the majorization context. For a given bipartite state ρ_{AB} and N-valued measurement X on A and X' on B, we denote the joint probability distribution of X and X' as $[\vec{p}^{(1)}(x), \vec{p}^{(2)}(x), \ldots, \vec{p}^{(N)}(x)]$, with the vector $\vec{p}^{(i)}(x)$ representing the probability distribution of measuring X on A conditioned on measuring X' on B and obtaining x'_i. We then define the majorized marginal distribution as

$$\vec{p}(x|x') \equiv \vec{p}^{(1)\downarrow}(x) + \vec{p}^{(2)\downarrow}(x) + \cdots + \vec{p}^{(N)\downarrow}(x), \tag{5}$$

where the superscript "$\downarrow$" in $\vec{p}^{(1)\downarrow}(x)$ indicates that the elements of vector $\vec{p}^{(i)}(x)$ are resorted in a nonincreasing order. For two pairs of measurements, the majorization relation $\vec{p}(x|x'_2) \prec \vec{p}(x|x'_1)$ means that X has less uncertainty conditioned on the X'_1 than X'_2.

Due to the majorization lattice theory [22–24], for a given ρ_{AB}, there exists a least upper bound for the majorized marginal distribution of X conditioned on any X', i.e.,

$$\forall X', \vec{p}(x|x') \prec \vec{s}. \tag{6}$$

Here, $\vec{s} = \vec{p}(x|x'_1) \vee \vec{p}(x|x'_2) \vee \cdots \vee \vec{p}(x|x'_N)$ depends only on the measurement X and the state, and is determined by implementing the join operator "$\vee$" of the majorization lattice (see Supplemental Material [25] for detailed discussions); $\vec{p}(x|x'_k)$ [defined as Eq. (5)] is the majorized marginal distribution of X conditioned on the kth measurement of the set $\{X'_k|k = 1, \ldots, N\}$. Each X'_k from the set gives a $\vec{p}(x|x'_k)$ that has the largest sum of the first k elements, i.e., $\sum_{i=1}^{k} p_i(x|x'_k) = \max_{\{X'\}}\{\sum_{i=1}^{k} p_i(x|x')\}$, with $p_i(x|x'_k)$ denoting the ith element of $\vec{p}(x|x'_k)$. The set $\{X'_k|k = 1, \ldots, N\}$ is thus the optimal measurement strategy for B to reduce the uncertainty of X on A.

For two measurements X and Y on A, a family of CMURs [24] is obtained,

$$\vec{p}(x|x') * \vec{p}(y|y') \prec \vec{s}^{(*)}, \tag{7}$$

with $\vec{s}^{(*)} = \vec{s}_x * \vec{s}_y$ ($* \in \{\otimes, \oplus, +\}$) [26]. Note that the CMUR in (7) can be directly generalized to an arbitrary number of observables. Unlike variance and entropic uncertainty relations, which are scalar measures of uncertainty, the CMURs provide a vectorized uncertainty measure of the uncertainty relations.

Experimental investigation of the CMURs. In our experiment, we detect the CMUR bound that violates the local uncertainty relation (4) in the presence of quantum memory, and then compare it with the CEUR bound given by the conditional entropic uncertainty relation (3).

Here, we consider the direct-sum version of the CMUR $\vec{p}(x|x') \oplus \vec{p}(y|y') \prec \vec{s}^{(\oplus)}$. A family of bipartite states $|\psi_\xi\rangle = \cos\xi|00\rangle + \sin\xi|11\rangle$ and the local measurements $X = \sigma(\theta, 0)$ and $Y = \sigma(\theta, \pi)$ are considered, where $\sigma(\theta, \phi) = \sigma_z \cos\theta + \sigma_x \sin\theta \cos\phi + \sigma_y \sin\theta \sin\phi$. The optimal measurement on B is then $\sigma' \equiv \sigma(\theta', \phi')$ with $\tan\theta' = \tan\theta \sin 2\xi$ and $\phi' = \phi$. Then we have $\vec{p}(\sigma|\sigma') \prec \vec{s}_\sigma = \begin{pmatrix} \frac{1}{2} + \frac{1}{2}\sqrt{\cos^2\theta + \sin^2\theta \sin^2 2\xi} \\ \frac{1}{2} - \frac{1}{2}\sqrt{\cos^2\theta + \sin^2\theta \sin^2 2\xi} \end{pmatrix}$.

As illustrated in Fig. 1, entangled photon pairs are generated via the type-I spontaneous parametric down-conversion process and are generated in the state $|\psi_\xi\rangle$ with visibilities higher than 97% [27,28].

In the experiments, ξ are chosen to be $\{\pi/4, \pi/8, \pi/16, 0\}$ resulting in the states varying from maximally entangled to separable. One of the photons in an entangled pair acts as a quantum memory [12]. The majorized marginal distribution $\vec{p}(x|x')$ [$\vec{p}(y|y')$] can be straightforwardly obtained from the probability distributions of the joint projection measurements X and X' (Y and Y') on A and B, respectively (see Table S1 in Supplemental Material [25] for details).

The CMURs are presented by Lorenz curves as majorization has an elegant geometric formulation involving the ordering of the Lorenz curves of two probability vectors [29]. For two given probability distributions $\vec{a}$ and $\vec{b}$, if the Lorenz curve of probability distribution $\vec{b}$ lies completely above that of $\vec{a}$, it implies $\vec{a} \prec \vec{b}$. In Fig. 2(a), the experimental results of the CMURs are shown. The blue color scheme curves and symbols indicate the experimental results of $\vec{s}^{(\oplus)}$ for the states $|\psi_\xi\rangle$. The red curves and symbols are the theoretical predictions of $\vec{s}$ of (4) for single-qubit systems. Only the curve for the separated state with $\xi = 0$ lies completely below that of $\vec{s}$. For the entangled state with $\xi > 0$, the CMUR has the upper bound $\vec{s}^{(\oplus)} \not\prec \vec{s}$. That means, the quantum uncertainty in correlated systems is beaten by introducing the quantum memory and applying an optimal measurement strategy.

To quantify experimental data, we calculate the Kullback-Leibler divergence [30] from the experimental results ($\vec{s}^{(\oplus)}_{\text{expt.}}$) to the theoretical predictions ($\vec{s}^{(\oplus)}_{\text{th}}$), which is defined as $D(P||Q) = \sum_i P(i) \log_2 \frac{P(i)}{Q(i)}$ for two probability distributions

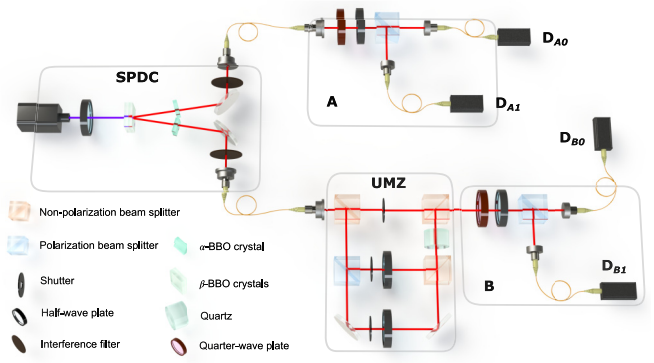

FIG. 1. Experimental setup. Photon pairs shared by A and B are generated in the state $|\psi_\xi\rangle$ via a type-I spontaneous parametric down-conversion process by pumping two adjacent nonlinear crystals (β-barium borate, BBO) with a 405-nm laser diode. The parameter ξ is set by the half-wave plate (HWP) in front of the BBO crystals. Two α-BBO crystals are inserted to compensate for the walk-off effect. Two interference filters restrict the photon bandwidth to 3 nm. Mixed states are prepared by letting one of the photons pass through the unbalanced Mach-Zehnder interferometer (UMZI). In the UMZI, two beam splitters first split the photon into three paths and then recombine them into one. Coherence in two of the arms is completely destroyed by inserting a quartz. The parameter p is controlled by manipulating the adjustable shutters. Local measurements on A and B are carried out via a sequence of a quarter-wave plate (QWP), an HWP, and a polarizing beam splitter (PBS) on each side, respectively. Coincidence measurements are then performed by avalanche photodiodes (APDs).

P and Q. For our experiment, all the values of $D(\vec{s}_{\text{th}}^{(\oplus)}||\vec{s}_{\text{expt.}}^{(\oplus)})$ are smaller than 0.1 (0 for a perfect match and 1 for a complete mismatch). That means, the experimental results agree well with their theoretical predictions.

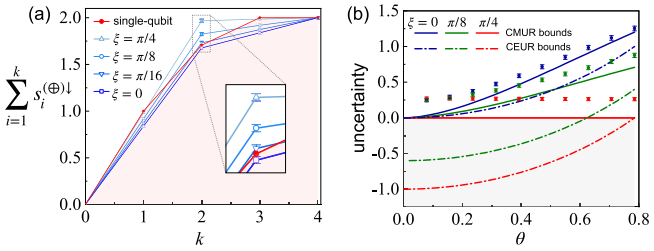

FIG. 2. Experimental results of the CMUR in the presence of quantum memory. (a) Upper bounds $\vec{s}^{(\oplus)}$ of the CMURs for observables $\{X = \sigma(\theta, 0), Y = \sigma(\theta, \pi)\}$ and the state $|\psi_\xi\rangle$ with $\theta = \pi/4$ and different ξ illustrated by Lorenz curves. Blue color scheme curves denote the theoretical predictions of the bounds $\vec{s}^{(\oplus)}$ and symbols for the corresponding experimental results, which violate the limit $\vec{s}$ for a single-particle system, represented by the red curve. (b) Lower bounds for CMUR and conditional entropic uncertainty relation (3) with quantum memory for different states. The solid curves indicate the theoretical predictions of the reduced lower bounds of $H(\vec{s}^{(\otimes)})$ and the symbols are for the experimental results. The dotted lines represent the CEUR bounds $[\log_2 \frac{1}{c} + S(A|B)]$. Error bars indicate the statistical uncertainty which is obtained via the Monte Carlo simulation method by assuming Poissonian photon-counting statistics.

Now we compare the CMUR to the conditional entropic uncertainty relation (3) in the presence of quantum memory. First, we calculate the Shannon entropy $H(\cdot)$ of both sides of the direct product form of the CMUR and transform it into an entropic form,

$$H(\vec{p}(x|x')) + H(\vec{p}(y|y')) \geqslant H(\vec{s}^{(\otimes)}), \tag{8}$$

where $\vec{s}^{(\otimes)} = \vec{s}_x \otimes \vec{s}_y$. The inequality is preserved because $H(\cdot)$ is a Schur-concave function. Then, with such a scalar measure version of the CMUR, the comparison between the two relations can be made. For the measurement on A, we choose $X = \sigma(\theta, 0), Y = \sigma(\theta, \pi)$ with $\theta \in \{\pi/40, \pi/20, \ldots, \pi/4\}$, and the optimal measurements X' and Y' on the quantum memory (B). Then the entropy can be obtained from the outcomes of the joint projection measurement for each pair of observables.

The experimental results of (8) are plotted in Fig. 2(b). The theoretical values of the CEUR bounds are denoted by dotted lines. The bound of the CMUR, as one can observe, is tighter than the corresponding CEUR bound. There are cases where CEUR bounds are negative, which are trivial since the lhs of the uncertainty relation (3) can never be negative as we discussed earlier in the Introduction. In contrast, the CMUR bounds are non-negative, and more importantly, physically reachable (via the optimal measurement strategy).

Steering criterion from CMURs. In the following, we demonstrate CMURs' advantages in steering detection. Many steering detection methods were motivated by concepts of entanglement detection [31]. Linear steering inequalities [32,33] are analogies to entanglement witnesses [34–38]. Similarly, steering criteria from uncertainty relations in terms of variances [39–42], entropy [43–47], and majorization (our method), share the same underlying idea with those for entanglement detection [12,16,48–55]. When quantum state tomography (QST) is available, there are quantification methods [56–59]. In addition, the question of steerability for a given special scenario (if measurements on A and conditional states of B are known) can be formulated as a semidefinite program (SDP) [60–71]. SDP demonstrates the advantage in determining if there admits a local hidden state (LHS) model [72–75]. Numerical methods are naturally restricted to cases with low dimensions and a few measurement settings due to exponentially increasing computational resource requests [76].

Our steering criterion is constructed based on the sum form of the CMUR, $\sum_{i=1}^{M} \vec{p}(x_i|x_i') \prec \vec{s}^{(+)}$, where $\vec{s}^{(+)} = \sum_{i=1}^{M} \vec{s}^{(x_i)}$ and M denotes the number of the observables. For single-particle systems, the majorization uncertainty relation is given by $\sum_{i=1}^{M} \vec{p}(x_i) \prec \vec{\epsilon}$ [22,24], where $\vec{\epsilon}$ is the aggregation [77] of $\vec{s}$ with $\epsilon_i = \sum_{j=1}^{M} s_{(i-1)*M+j}$. Then we have the following proposition:

Proposition 1 (steering criterion from CMURs). A bipartite state is steerable if the inequality

$$\vec{s}^{(+)} \prec \vec{\epsilon} \tag{9}$$

is violated. Here, $\vec{s}^{(+)}$ is the CMUR bound in its sum form and $\vec{\epsilon}$ is the bound of the majorization uncertainty relation for single-particle systems.

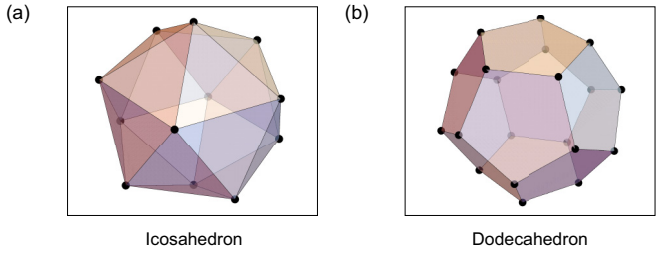

FIG. 3. Illustration of the measurement-setting choices. We take the Bloch-space directions through antipodal pairs of vertices of Platonic polyhedra as axes for measurement. (a) Icosahedron for $M = 6$. (b) Dodecahedron for $M = 10$.

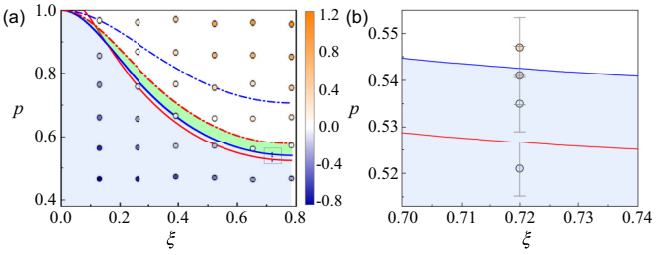

FIG. 4. Experimental results of the steerability of the states ρ_ξ. (a) Distribution of experimental states. The blue and red curves represent the theoretical predictions of states ρ_ξ when $\vec{s}^{(+)} = \vec{\epsilon}$ for the case of six and ten measurement settings, respectively. The symbols under the blue (red) curve (in the light blue area) indicate that A cannot steer B. The dots above the blue (red) curve indicate that A can steer B. Dot textures are colored according to the degree of the violation. The blue and red dotted lines represent the theoretical predictions for the case of two and three settings, respectively. For the states in the green area, steerability can only be observed for six settings (of our method) but failed for both two and three settings (former methods). (b) A larger version of the blue dotted box in (a) to show more details.

See Supplemental Material [25] for the proof.

As the CMUR is applicable to an arbitrary number of observables, this enables us to study steerability with any number of settings, which is usually a tough task for variance- and entropy-based uncertainty relations. With the straightforward optimal measurement strategy (which maximally violates the criterion), our method can be efficiently implemented for an arbitrary number of settings, leading to low costs in classical computation and experimental resources.

In the experiment, we demonstrate the majorized steering criterion on a family of weakly steerable (i.e., one-way steerable) states [78]: $\rho_\xi = (1-p)/2\rho_\xi^A \otimes I + p|\psi_\xi\rangle\langle\psi_\xi|$. Here, $\rho_\xi^A = \mathrm{Tr}_B(|\psi_\xi\rangle\langle\psi_\xi|)$ and $p \in [0, 1]$. The optimal measurements strategy $[X' = \sigma'(\theta', \phi')$ with $\tan\theta' = \tan\theta\sin(2\xi)$ and $\phi' = -\phi]$ is performed on A to reduce the measurement uncertainty of B $[X = \sigma(\theta, \phi)]$. If the corresponding bound $\vec{\epsilon}$ of X for a single-particle system is violated by $\vec{s}^{(+)}$, i.e., inequality (9) is detected to be violated, we say A can steer B.

We take the axes of the antipodal vertices of the Platonic icosahedron (dodecahedron) as the directions for the cases of $M = 6$ (10) measurement settings as illustrated in Fig. 3. The majorized marginal distribution $\vec{p}(x_i|x_i')$ of each observable is then measured (see Supplemental Material [25] for more experimental details) with the optimal measurement strategy to obtain the bound $\vec{s}^{(+)}$.

The aggregation $\vec{\epsilon}$ of the single-particle system can be theoretically obtained by the method introduced in Refs. [22,79]. For the cases of six and ten observables, the first element of $\vec{\epsilon}$ (the largest element) is $\epsilon_1 = 1 + 5\cos^2[1/2\arccos(1/\sqrt{5})]$ and $\epsilon_1 = 1 + 6\cos^2[1/2\arccos(1/3)]^2 + 3\cos^2[1/2\arccos(0.7454)]$, respectively. We then compare ϵ_1 with the first element of $\vec{s}^{(+)}$ to determine whether the criterion (9) is violated, thus verifying the steerability.

A total of 36 states ρ_ξ with different parameter pairs p and ξ are tested (see Supplemental Material [25] for more experimental details). The experimental results are shown in Fig. 4. The blue and red curves are the bounds of the CUMRs and $\vec{s}^{(+)} = \vec{\epsilon}$ for six and ten observables, respectively. The symbols under the blue (red) curve indicate that A cannot steer B, while for those states above the blue (red) curve, A can steer B. Dot textures are colored according to the degree of the violation (the first element of $\vec{s}^{(+)}$ minus that of $\vec{\epsilon}$). We also plot the theoretical predictions for two and three settings in dotted lines in Fig. 4(a) for comparison. Below the two dotted lines but above the blue curves is the area (colored in green) where steerability can only be observed for six settings (our method) but failed for both two and three settings. The adopted quantification method (steering radius [57,58]) requires the use of QST and involves solving the equation set [59] with an exponentially increasing size with respect to the number of settings. It is also worth mentioning that the seminal results in Ref. [33] show that steering can be demonstrated with Bell local states. In the experiments they deployed the linear inequality [32] for steering detection, using up to six measurement settings. Efforts have since been made [80] in deploying further this criterion for cases of a larger number of settings. In these regards, our method can be regarded as a complementary progress to these methods, since it can be implemented for an arbitrary number of settings without solving problems with exponentially increasing complexity. Our method does not request QST. With our method, the experimental cost increases linearly with the number of settings. These allow an improvement of the detection capability by performing additional measurements. Please note that the underlying concepts of these methods are essentially different (see Supplemental Material [25] for more discussions).

Conclusion. In this Letter, we report an experimental investigation of the CMURs in the presence of quantum memory in a photonic system. The vectorized measure results afford glimpses into the lattice structures of quantum uncertainty and quantum correlations, which are usually studied with scalar measures. Most importantly, we experimentally show that the bound given by the new uncertainty relations is physically reachable and nontrivial, whereas the previous CEUR bound may be physically unreachable and hence trivial when the system is strongly entangled. As an application, we demonstrated the advantages of CMUR in witnessing steerability. The proposed criterion applies to an arbitrary number of measurement settings and requires low classical computation and experimental resources. This offers a practical way for the quantitative investigation of steerability on a more accurate

level. We therefore expect the CMURs in the presence of quantum memory to have further use both in quantum information theory and beyond.

Acknowledgments. This work has been supported by the NSFC (Grant No. 92265209, No. 12025401, and No. 11635009).

[1] W. Heisenberg, Z. Phys. **43**, 172 (1927).
[2] H. P. Robertson, Phys. Rev. **34**, 163 (1929).
[3] D. Qu, K. Wang, L. Xiao, X. Zhan, and P. Xue, Opt. Express **29**, 29567 (2021).
[4] L. Xiao, B. Fan, K. Wang, A. K. Pati, and P. Xue, Phys. Rev. Res. **2**, 023106 (2020).
[5] B. Fan, K. Wang, L. Xiao, and P. Xue, Phys. Rev. A **98**, 032118 (2018).
[6] P. Xue, B. Fan, K. Wang, and L. Xiao, Proc. SPIE **10771**, 1077110 (2018).
[7] L. Xiao, K. Wang, X. Zhan, Z. Bian, J. Li, Y. Zhang, P. Xue, and A. K. Pati, Opt. Express **25**, 17904 (2017).
[8] D. Deutsch, Phys. Rev. Lett. **50**, 631 (1983).
[9] K. Kraus, Phys. Rev. D **35**, 3070 (1987).
[10] H. Maassen and J. B. M. Uffink, Phys. Rev. Lett. **60**, 1103 (1988).
[11] J. M. Renes and J.-C. Boileau, Phys. Rev. Lett. **103**, 020402 (2009).
[12] M. Berta, M. Christandl, R. Colbeck, J. M. Renes, and R. Renner, Nat. Phys. **6**, 659 (2010).
[13] Y.-H. Kim and Y. Shih, Found. Phys. **29**, 1849 (1999).
[14] M. D. Reid and P. D. Drummond, Phys. Rev. Lett. **60**, 2731 (1988).
[15] M. D. Reid, Phys. Rev. A **40**, 913 (1989).
[16] C.-F. Li, J.-S. Xu, X.-Y. Xu, K. Li, and G.-C. Guo, Nat. Phys. **7**, 752 (2011).
[17] I. Devetak and A. Winter, Proc. R. Soc. A **461**, 207 (2005).
[18] M. H. Partovi, Phys. Rev. A **84**, 052117 (2011).
[19] Z. Puchała, Ł. Rudnicki, and K. Życzkowski, J. Phys. A: Math. Theor. **46**, 272002 (2013).
[20] S. Friedland, V. Gheorghiu, and G. Gour, Phys. Rev. Lett. **111**, 230401 (2013).
[21] L. Rudnicki, Z. Puchała, and K. Życzkowski, Phys. Rev. A **89**, 052115 (2014).
[22] J.-L. Li and C.-F. Qiao, Ann. Phys. **531**, 1900143 (2019).
[23] F. Cicalese and U. Vaccaro, IEEE Trans. Inf. Theory **48**, 933 (2002).
[24] J.-L. Li and C.-F. Qiao, Adv. Quantum. Technol. **3**, 2000039 (2020).
[25] See Supplemental Material at http://link.aps.org/supplemental/10.1103/PhysRevA.108.L050202 for details on the optimal measurement strategy to reduce local uncertainty via the majorization lattice, CMUR criterion for witnessing steerability and the proof, experimental details, as well as a comparison with other steering criterions.
[26] G. Gour, A. Grudka, M. Horodecki, W. Kłobus, J. Łodyga, and V. Narasimhachar, Phys. Rev. A **97**, 042130 (2018).
[27] Y. Nambu, K. Usami, Y. Tsuda, K. Matsumoto, and K. Nakamura, Phys. Rev. A **66**, 033816 (2002).
[28] G. Akselrod, J. Altepeter, E. Jeffrey, and P. G. Kwiat, Opt. Express **15**, 5260 (2007).
[29] M. O. Lorenz, Am. Stat. Assoc. **9**, 209 (1905).
[30] T. M. Cover, *Elements of Information Theory* (Wiley, Hoboken, NJ, 1999).
[31] O. Gühne and G. Tóth, Phys. Rep. **474**, 1 (2009).
[32] E. G. Cavalcanti, S. J. Jones, H. M. Wiseman, and M. D. Reid, Phys. Rev. A **80**, 032112 (2009).
[33] D. J. Saunders, S. J. Jones, H. M. Wiseman, and G. J. Pryde, Nat. Phys. **6**, 845 (2010).
[34] M. Horodecki, P. Horodecki, and R. Horodecki, Phys. Lett. A **223**, 1 (1996).
[35] B. M. Terhal, Phys. Lett. A **271**, 319 (2000).
[36] B. M. Terhal, Theor. Comput. Sci. **287**, 313 (2002).
[37] M. Barbieri, F. De Martini, G. Di Nepi, P. Mataloni, G. M. D'Ariano, and C. Macchiavello, Phys. Rev. Lett. **91**, 227901 (2003).
[38] P. Krammer, H. Kampermann, D. Bruß, R. A. Bertlmann, L. C. Kwek, and C. Macchiavello, Phys. Rev. Lett. **103**, 100502 (2009).
[39] R. Uola, A. C. S. Costa, H. C. Nguyen, and O. Gühne, Rev. Mod. Phys. **92**, 015001 (2020).
[40] S. P. Walborn, A. Salles, R. M. Gomes, F. Toscano, and P. H. Souto Ribeiro, Phys. Rev. Lett. **106**, 130402 (2011).
[41] A. C. S. Costa, R. Uola, and O. Gühne, Phys. Rev. A **98**, 050104(R) (2018).
[42] J. Schneeloch, C. J. Broadbent, S. P. Walborn, E. G. Cavalcanti, and J. C. Howell, Phys. Rev. A **87**, 062103 (2013).
[43] Y.-Z. Zhen, Y.-L. Zheng, W.-F. Cao, L. Li, Z.-B. Chen, N.-L. Liu, and K. Chen, Phys. Rev. A **93**, 012108 (2016).
[44] A. Costa, R. Uola, and O. Gühne, Entropy **20**, 763 (2018).
[45] J. Schneeloch, P. B. Dixon, G. A. Howland, C. J. Broadbent, and J. C. Howell, Phys. Rev. Lett. **110**, 130407 (2013).
[46] A. Riccardi, C. Macchiavello, and L. Maccone, Phys. Rev. A **97**, 052307 (2018).
[47] T. Kriváchy, F. Fröwis, and N. Brunner, Phys. Rev. A **98**, 062111 (2018).
[48] W. P. Bowen, R. Schnabel, P. K. Lam, and T. C. Ralph, Phys. Rev. Lett. **90**, 043601 (2003).
[49] H. F. Hofmann and S. Takeuchi, Phys. Rev. A **68**, 032103 (2003).
[50] O. Gühne, Phys. Rev. Lett. **92**, 117903 (2004).
[51] J. C. Howell, R. S. Bennink, S. J. Bentley, and R. W. Boyd, Phys. Rev. Lett. **92**, 210403 (2004).
[52] R. Prevedel, D. R. Hamel, R. Colbeck, K. Fisher, and K. J. Resch, Nat. Phys. **7**, 757 (2011).
[53] O. Gühne and M. Lewenstein, Phys. Rev. A **70**, 022316 (2004).
[54] L. Maccone, D. Bruß, and C. Macchiavello, Phys. Rev. Lett. **114**, 130401 (2015).
[55] D. Sauerwein, C. Macchiavello, L. Maccone, and B. Kraus, Phys. Rev. A **95**, 042315 (2017).
[56] M. Piani and J. Watrous, Phys. Rev. Lett. **114**, 060404 (2015).
[57] K. Sun, X.-J. Ye, J.-S. Xu, X.-Y. Xu, J.-S. Tang, Y.-C. Wu, J.-L. Chen, C.-F. Li, and G.-C. Guo, Phys. Rev. Lett. **116**, 160404 (2016).

[58] Y. Xiao, X.-J. Ye, K. Sun, J.-S. Xu, C.-F. Li, and G.-C. Guo, Phys. Rev. Lett. **118**, 140404 (2017).
[59] C. Wu, J.-L. Chen, X.-J. Ye, H.-Y. Su, D.-L. Deng, Z. Wang, and C. H. Oh, Sci. Rep. **4**, 4291 (2014).
[60] T. Moroder, O. Gittsovich, M. Huber, and O. Gühne, Phys. Rev. Lett. **113**, 050404 (2014).
[61] M. T. Quintino, T. Vértesi, and N. Brunner, Phys. Rev. Lett. **113**, 160402 (2014).
[62] R. Uola, T. Moroder, and O. Gühne, Phys. Rev. Lett. **113**, 160403 (2014).
[63] P. Skrzypczyk, M. Navascués, and D. Cavalcanti, Phys. Rev. Lett. **112**, 180404 (2014).
[64] H. Zhu, M. Hayashi, and L. Chen, Phys. Rev. Lett. **116**, 070403 (2016).
[65] I. Kogias, P. Skrzypczyk, D. Cavalcanti, A. Acín, and G. Adesso, Phys. Rev. Lett. **115**, 210401 (2015).
[66] D. Cavalcanti, L. Guerini, R. Rabelo, and P. Skrzypczyk, Phys. Rev. Lett. **117**, 190401 (2016).
[67] F. Hirsch, M. T. Quintino, T. Vértesi, M. F. Pusey, and N. Brunner, Phys. Rev. Lett. **117**, 190402 (2016).
[68] S. T. Ali, C. Carmeli, T. Heinosaari, and A. Toigo, Found. Phys. **39**, 593 (2009).
[69] J. Bowles, T. Vértesi, M. T. Quintino, and N. Brunner, Phys. Rev. Lett. **112**, 200402 (2014).
[70] D. Cavalcanti and P. Skrzypczyk, Rep. Prog. Phys. **80**, 024001 (2017).
[71] M. F. Pusey, Phys. Rev. A **88**, 032313 (2013).
[72] H. M. Wiseman, S. J. Jones, and A. C. Doherty, Phys. Rev. Lett. **98**, 140402 (2007).
[73] J. Barrett, Phys. Rev. A **65**, 042302 (2002).
[74] M. T. Quintino, T. Vértesi, D. Cavalcanti, R. Augusiak, M. Demianowicz, A. Acín, and N. Brunner, Phys. Rev. A **92**, 032107 (2015).
[75] J. Bowles, F. Hirsch, M. T. Quintino, and N. Brunner, Phys. Rev. Lett. **114**, 120401 (2015).
[76] M. Fillettaz, F. Hirsch, S. Designolle, and N. Brunner, Phys. Rev. A **98**, 022115 (2018).
[77] F. Cicalese, L. Gargano, and U. Vaccaro, IEEE Trans. Inf. Theory **65**, 3436 (2019).
[78] J. Bowles, F. Hirsch, M. T. Quintino, and N. Brunner, Phys. Rev. A **93**, 022121 (2016).
[79] J.-L. Li and C.-F. Qiao, Quantum Inf. Process. **20**, 109 (2021).
[80] Y.-L. Zheng, Y.-Z. Zhen, W.-F. Cao, L. Li, Z.-B. Chen, N.-L. Liu, and K. Chen, Phys. Rev. A **95**, 032128 (2017).